44. Condition-Based Failure Prediction

Machine reliability is improved if failures are prevented. Preventive maintenance (PM) can be performed in order to promote reliability, but only if failures can be predicted early enough. Although PM can be approached in different ways, according to time or condition, whichever one of these approaches is adopted, the key issue is whether a failure can be detected early enough or even predicted. This chapter discusses a way to predict failure, for use with PM, in which the state of a DC motor is estimated using the Kalman filter. The prediction consists of a simulation on a computer and an experiment performed on the DC motor. In the simulation, an exponential attenuator is placed at the output end of the motor model in order to simulate aging failure. Failure is ascertained by monitoring a state variables, the rotation speed of the motor. Failure times were generated by Monte Carlo simulation and predicted by the Kalman filter. One-step-ahead and two-steps-ahead predictions are performed. The resulting prediction errors are sufficiently small in both predictions. In the experiment, the rotating speed of the motor was measured every 5 min for 80 days. The measurements were used to perform Kalman prediction and to verify the prediction accuracy. The resulting prediction errors were acceptable. Decreasing the increment time between measurements was found to increase the accuracy of Kalman prediction uses. Consequently, it is shown that failure can be prevented (promoting reliability) by performing predictive maintenance depending on the results of state estimation using the Kalman filter.

Nomenclature

$(\cdot)_k$	= The value of $(\cdot)$ at time kT
$\widehat{(\cdot)}_{a/b}$	= The estimate of $(\cdot)$ at time aT based on all information known about the process up to time bT
$\boldsymbol{A}$	= A matrix
$\boldsymbol{A}_\mathrm{c}$	= Coefficient matrix of the state equation for a continuous system
$\boldsymbol{A}_\mathrm{d}$	= Coefficient matrix of the state equation for a discrete system
$\boldsymbol{A}^\mathrm{T}$	= Transpose matrix of $\boldsymbol{A}$
$\boldsymbol{A}^{-1}$	= Inverse matrix of $\boldsymbol{A}$
B	= Damping coefficient
$\boldsymbol{B}_\mathrm{c}$	= Coefficient matrix of the state equation for a continuous system
$\boldsymbol{B}_\mathrm{d}$	= Coefficient matrix of the state equation for a discrete system
$\boldsymbol{B}_\mathrm{k}$	= Coefficient matrix for the input term of a discrete state equation
$\boldsymbol{C}$	= A matrix
$\boldsymbol{C}_\mathrm{c}$	= Coefficient matrix of the state equation for a continuous system
$\boldsymbol{C}_\mathrm{d}$	= Coefficient matrix of the state equation for a discrete system

$\boldsymbol{D}_{\mathrm{c}}$ = Coefficient matrix of the state equation for a continuous system
$\boldsymbol{D}_{\mathrm{d}}$ = Coefficient matrix of the state equation for a discrete system
E = Applied voltage
E_r = Estimation error
$\boldsymbol{H}_{\mathrm{k}}$ = Matrix giving the ideal (noiseless) connection between the measurement and the state vector
i_{a} = Armature winding current
J = Moment of inertia of rotor and load
k_{b} = Back emf constant
K_{k} = Kalman gain
k_{T} = Motor torque constant
L_{a} = Armature winding inductance
L^{-1} = The inverse Laplace transform
$\boldsymbol{P}_{k/k-1}$ = Estimation error covariance matrix
$\boldsymbol{Q}_k$ = Covariance matrices for disturbance
R = Armature winding resistance
$\boldsymbol{R}_k$ = Covariance matrices for noise
t = Time variable
T = Motor output torque
T = Increment time for every step in Kalman prediction
$\boldsymbol{U}_k$ = Control input of a discrete state equation at state k
V = Variation in the estimated rotating speed
$\boldsymbol{V}_k$ = Noise (measurement error vector), assumed to be a white sequence with known covariance
$\boldsymbol{W}_k$ = Disturbance (system stochastic input vector), assumed to be a white sequence with known covariance and zero cross-correlation with V_k sequence
x, X = Variable of a distribution function
$\boldsymbol{X}_{D0}$ = Initial states resulting from deterministic input
$\boldsymbol{X}_k$ = System state vector at state k
$\boldsymbol{X}_{S0}$ = Initial states resulting from stochastic input
$\boldsymbol{Y}_k$ = System output vector at state k
Z_k = Output measurement vector
θ = Motor angle displacement
$\dot{\theta}$ = Motor rotating speed
μ = Mean value of a distribution function
σ = Standard deviation of a distribution function
Φ_k = Matrix relating $\boldsymbol{X}_k$ to $\boldsymbol{X}_{k+1}$ in the absence of a forcing function, which is the state transition matrix if $\boldsymbol{X}_k$ is sampled from a continuous process

44.1 Overview

High quality and excellent performance of a system are always goals that engineers strive to achieve. Reliability engineering encourages system quality and performance from the beginning to the end of the system's lifecycle [44.1]. Therefore, reliability can be thought of as the time-dimensional quality of the system. Reliability is affected by every stage of the system's lifecycle, including its development, design, production, quality control, shipping, installation, operation, and maintenance. Consequently, paying attention to each of the stages promotes reliability. Specifically, in the onsite operation phase, failures are the main causes of worsened performance and degraded reliability. This is a very important consideration for any equipment that may cause severe damage to public safety or financial benefit upon failure, such as nuclear power plants, passenger vehicles, or semiconductor production lines. Accordingly, failure avoidance is the main approach to ensuring reliability. Effective maintenance is the best way to reduce failure [44.1]. There are three main types of maintenance: improvement maintenance (IM), corrective maintenance (CM), and preventive maintenance (PM) [44.2]. The purpose of IM is to reduce the need for maintenance or eliminate the need for it entirely . Therefore IM should be performed at the design phase of a system in order to emphasize the elimination of failure. There are many restrictions on a designer, however, such as space, budget, and market requirements. Usually the reliability of a product is related to its price.

On the other hand, CM is the repair performed after failure occurs, while PM refers to all of the actions intended to maintain equipment in good operating condition and to avoid failure [44.2]. The most common strategy for maintenance is scheduled maintenance, where maintenance occurs at set times, at set operational times, after set amounts of material have been processed, or by some other prescribed criteria. Nevertheless, there are at least two drawbacks to this type of maintenance:

1. The criteria on which the scheduled maintenance is based are statistical averages, such as mean time to failure (MTTF). This leads to an unavoidable risk that a system can fail before the criteria are exceeded; in other words a failure may occur unexpectedly.
2. The real duty cycles for certain parts or modules may be longer than those averages, but they are still replaced during a scheduled maintenance, which is wasteful.

In contrast, condition monitoring is a more reasonable type of maintenance than scheduled maintenance. However, a failure really needs to be detected prior to its occurrence.

The relationship between error, failure, and fault is illustrated in Fig. 44.1, and the three terms are defined as follows [44.3]:

1. An error is a discrepancy between a computed, observed or measured value or condition and the true, specified or theoretically correct value or condition.
2. Failure is an event where a required function is terminated (exceeding the acceptable limits).
3. Fault is the state characterized by an inability to perform a required function, excluding the inability encountered during preventive maintenance or other planned actions, or due to lack of external resources.

Based on the above statements, an error is not a failure and a fault is hence a state resulting from a failure. An error is sometimes referred to as an incipient failure [44.4]. Therefore, PM action is taken when the system is still at an error condition – within acceptable deviation and before failure occurs. Hence, PM is an effective approach to promoting reliability [44.5]. As mentioned before, time-based and condition-based maintenance are two major approaches to PM. Irrespective of the approach adopted for PM, the key issue is whether a failure can be detected early or even predicted.

Many methods have been proposed for failure prediction, such as statistical knowledge of the reliability parameters [44.6, 7], neural network studies [44.8], and understanding the failure mechanism of damaged products [44.9]. Fault detection based on modeling and estimation is one of these methods [44.10]. The Kalman filter is useful not only for state estimation but also for

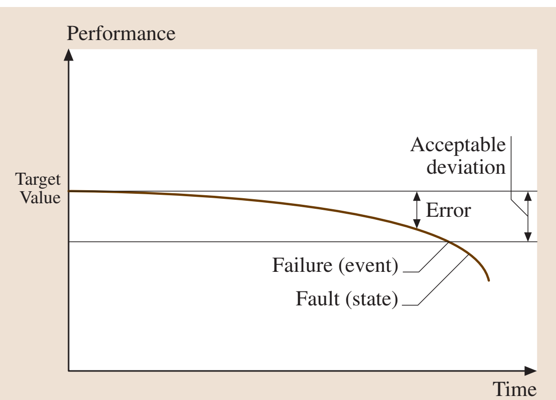

Fig. 44.1 Error, failure and fault

state prediction. It has been widely used in different fields over the past few decades, such as in on-line failure detection [44.11], real-time prediction of vehicle motion [44.12], and prediction of maneuvering target trajectories [44.13]. The Kalman filter is a linear, discrete-time, and finite-dimensional system [44.14]. Its appearance is a copy of the system that is estimated. Inputs to the filter include the control signal and the difference value between measured and estimated state variables. Actual values of the event acquired by the monitor sensor are fed into the corresponding Kalman filter to execute state estimation. By minimizing mean-square estimation errors, an optimal estimate can be derived. Using the current state, the Kalman filter provides a predicted value of the next state for the corresponding event at every time interval T. As a result, the output of the filter becomes optimal estimates of the state variables for the next time step. Each event has a prescribed failure threshold, and the predicted value is compared with the prescribed failure threshold in order to judge whether the monitored event has failed after T or is still within the established threshold. Once the estimated value reaches the threshold, failure is predicted. Therefore, the current state is a warning state and PM needs to be performed. If predicted state variables indicate that a device is going to fail, then the failure can be prevented in time using PM. However, future state variables need to be accurately predicted a reasonable time before failure occurrence [44.10, 15].

This chapter is about state estimation and how to predict the need for PM using a Kalman filter. A DC motor is the object on which we perform condition-based failure predictions. The prediction consists of two parts. The first part is a simulation on a computer, and the second part is an experiment on the DC motor. In the simulation, failure times were generated by Monte Carlo simulation (MCS) and predicted by the Kalman filter. One-step-ahead and two-steps-ahead predictions were conducted. The resulting prediction errors are sufficiently small in both predictions. Even so, the failure prediction was still simulated on a computer. In the second part of the prediction, a DC motor and a data acquisition system are used to implement the simulation. The rotation speed of the motor is chosen as the major state variable to judge whether the motor is going to fail, by estimating state using the Kalman filter. The rotation speed of the motor was measured and recorded every 5 min for 80 d. Instead of simulated data, the measured data are used to perform Kalman prediction and to verify the prediction accuracy.

In Sect. 44.2, we study a discrete system model with deterministic control input, white noise disturbance and noisy output measurement. We then formulate an equation for state estimation of the Kalman filter. Deterministic inputs are considered in this formulation. Moreover, equations for N-step-ahead prediction are derived. Section 44.3 presents the transfer function, the continuous state model, and the discrete state model of the DC motor that is employed as an example in this chapter. Section 44.4 presents a simulated system with prescribed parameters, a Monte Carlo simulation and an ARMA model used to generate necessary data for a failure prediction simulation, and the exponential attenuator used to simulate the aging failure mode. Simulation results are also given and discussed. Section 44.5 presents the experimental set-up with related parameters, experimental results and discussion. Section 44.6 concludes this work.

44.2 Kalman Filtering

This section introduces the Kalman filtering that is used in this chapter to perform the failure prediction.

44.2.1 System Model

The block diagram of a discrete system is shown in Fig. 44.2. The state equations [44.14] are:

$$\boldsymbol{X}_{k+1} = \boldsymbol{\Phi}_k \boldsymbol{X}_k + \mathbf{B}_k \boldsymbol{U}_k + \boldsymbol{W}_k \,, \tag{44.1}$$

$$\boldsymbol{Y}_k = \mathbf{H}_k \boldsymbol{X}_k \,, \tag{44.2}$$

$$\boldsymbol{Z}_k = \boldsymbol{Y}_k + \boldsymbol{V}_k \,. \tag{44.3}$$

Substituting (44.2) into (44.3) yields

$$\boldsymbol{Z}_k = \mathbf{H}_k \boldsymbol{X}_k + \boldsymbol{V}_k \,. \tag{44.4}$$

Let $E[\boldsymbol{X}]$ be the expected value of $\boldsymbol{X}$; therefore, the covariance matrices for $\boldsymbol{W}_k$ and $\boldsymbol{V}_k$ are given by:

$$E\left[\boldsymbol{W}_k \boldsymbol{W}_i^{\mathrm{T}}\right] = \begin{cases} \mathbf{Q}_k \,, & i = k \\ 0 \,, & i \neq k \end{cases} \tag{44.5}$$

$$E\left[\boldsymbol{V}_k \boldsymbol{V}_i^{\mathrm{T}}\right] = \begin{cases} \mathbf{R}_k \,, & i = k \\ 0, & i \neq k \end{cases} \tag{44.6}$$

$$E\left[\boldsymbol{W}_k \boldsymbol{V}_i^{\mathrm{T}}\right] = 0 \,, \quad \text{for all } k \text{ and } i \,. \tag{44.7}$$

It follows that both $\mathbf{Q}_k$ and $\mathbf{R}_k$ are symmetric and positive definite [44.16].

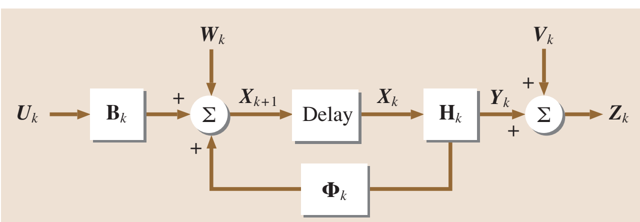

Fig. 44.2 Block diagram of a discrete system

44.2.2 State Estimation

State estimation involves guessing the value of $\boldsymbol{X}_k$ by using measured data, i. e. $Z_0, Z_1, \ldots \; Z_{k-1}$. Accordingly, $\hat{\boldsymbol{X}}_{k/k-1}$ is called the prior estimate of $\boldsymbol{X}$, and $\hat{\boldsymbol{X}}_{k/k}$ is called the posterior estimate of $\boldsymbol{X}$ [44.16]. The prior estimation error is defined as

$$\mathbf{e}_{k/k-1} = \boldsymbol{X}_k - \hat{\boldsymbol{X}}_{k/k-1} \,. \tag{44.8}$$

Since $\boldsymbol{W}_k$ and $\boldsymbol{V}_k$ are assumed to be white sequences, the prior estimation error has a mean of zero. Consequently, the associated error covariance matrix is written as

$$\begin{aligned} \boldsymbol{P}_{k/k-1} &= E\left[(\mathbf{e}_{k/k-1})(\mathbf{e}_{k/k-1})^{\mathrm{T}}\right] \\ &= E\left[(\boldsymbol{X}_k - \hat{\boldsymbol{X}}_{k/k-1})(\boldsymbol{X}_k - \hat{\boldsymbol{X}}_{k/k-1})^{\mathrm{T}}\right] . \end{aligned} \tag{44.9}$$

The estimation problem begins with no prior measurements. Thus, the stochastic portion of the initial estimate is zero if the stochastic process mean is zero; i. e. $\hat{\boldsymbol{X}}_{0/-1}$ is only driven by deterministic input X_{D0}. It follows from (44.8) that

$$e_{0/-1} = X_0 - \hat{\boldsymbol{X}}_{0/-1} = X_0 - X_{D0} = X_{S0} \,. \tag{44.10}$$

Employing (44.9) and (44.10) yields

$$P_{0/-1} = E\left[\boldsymbol{X}_{S0} \boldsymbol{X}_{S0}^{\mathrm{T}}\right] . \tag{44.11}$$

The Kalman filter is a copy of the original system and is driven by the estimation error and the deterministic input. The block diagram of the filter structure is shown in Fig. 44.3. The filter is used to improve the prior estimate to make it the posterior estimate via the measurement $\boldsymbol{Z}_k$. A linear blending of the noisy measurement and the prior estimate is written as [44.16]

$$\hat{\boldsymbol{X}}_{k/k} = \hat{\boldsymbol{X}}_{k/k-1} + \boldsymbol{K}_{\mathrm{k}}(\boldsymbol{Z}_k - \boldsymbol{H}_k \hat{\boldsymbol{X}}_{k/k-1}) \,, \tag{44.12}$$

where K_{k} is the blending factor for this structure. Once the posterior estimate is determined, the posterior estimation error and associated error covariance matrix can be derived as

$$\mathbf{e}_{k/k} = \boldsymbol{X}_k - \hat{\boldsymbol{X}}_{k/k}\,, \tag{44.13}$$

$$\begin{aligned}\boldsymbol{P}_{k/k} &= E[(\mathbf{e}_{k/k})(\mathbf{e}_{k/k})^T]\,,\\ &= E[(\boldsymbol{X}_k - \hat{\boldsymbol{X}}_{k/k})(\boldsymbol{X}_k - \hat{\boldsymbol{X}}_{k/k})^T]\,.\end{aligned} \tag{44.14}$$

The optimal blending factor is written as [44.16]

$$K_\mathrm{k} = \boldsymbol{P}_{k/k-1}\mathbf{H}_\mathrm{k}^\mathrm{T}(\mathbf{H}_k\boldsymbol{P}_{k/k-1}\mathbf{H}_\mathrm{k}^\mathrm{T} + \mathbf{R}_k)^{-1}\,. \tag{44.15}$$

This specific K_k, namely the one that minimizes the mean-square estimation error, is called the Kalman gain.

Substituting (44.15) into (44.12), the posterior error covariance matrix can be derived as follows:

$$\begin{aligned}\boldsymbol{P}_{k/k} &= \boldsymbol{P}_{k/k-1} - \boldsymbol{P}_{k/k-1}\mathbf{H}_k^\mathrm{T}\left(\mathbf{H}_k\boldsymbol{P}_{k/k-1}\mathbf{H}_k^\mathrm{T} + \mathbf{R}_k\right)^{-1}\\ &\quad\times\mathbf{H}_k\boldsymbol{P}_{k/k-1}\\ &= \boldsymbol{P}_{k/k-1} - \boldsymbol{K}_\mathrm{k}\left(\mathbf{H}_k\boldsymbol{P}_{k/k-1}\mathbf{H}_k^\mathrm{T} + \mathbf{R}_k\right)\boldsymbol{K}_\mathrm{k}^\mathrm{T}\\ &= (I - \boldsymbol{K}_\mathrm{k}\mathbf{H}_k)\boldsymbol{P}_{k/k-1}\,.\end{aligned} \tag{44.16}$$

As depicted in Fig. 44.3, the one-step-ahead estimate is formulated as

$$\begin{aligned}\hat{\boldsymbol{X}}_{k+1/k} &= \boldsymbol{\Phi}_k\hat{\boldsymbol{X}}_{k/k-1} + \boldsymbol{\Phi}_k\boldsymbol{K}_\mathrm{k}(Z_k - \boldsymbol{H}_k\hat{\boldsymbol{X}}_{k/k-1})\\ &\quad + \boldsymbol{B}_k\boldsymbol{U}_k\\ &= \boldsymbol{\Phi}_k[\hat{\boldsymbol{X}}_{k/k-1} + \boldsymbol{K}_\mathrm{k}(\boldsymbol{Z}_k - \boldsymbol{H}_k\hat{\boldsymbol{X}}_{k/k-1})]\\ &\quad + \boldsymbol{B}_k\boldsymbol{U}_k\\ &= \boldsymbol{\Phi}_k\hat{\boldsymbol{X}}_{k/k} + \boldsymbol{B}_k\boldsymbol{U}_k\,.\end{aligned} \tag{44.17}$$

Consequently, the one-step-ahead estimation error is derived as

$$\begin{aligned}\mathbf{e}_{k+1/k} &= (\boldsymbol{\Phi}_k\boldsymbol{X}_k + \mathbf{B}_k\boldsymbol{U}_k + \mathbf{W}_k) - (\boldsymbol{\Phi}_k\hat{\boldsymbol{X}}_{k/k} + \mathbf{B}_k\boldsymbol{U}_k)\\ &= \boldsymbol{\Phi}_k(\boldsymbol{X}_k - \hat{\boldsymbol{X}}_{k/k}) + \mathbf{W}_k\\ &= \boldsymbol{\Phi}_k\mathbf{e}_{k/k} + \mathbf{W}_k\,.\end{aligned} \tag{44.18}$$

In a manner similar to (44.14), the one-step-ahead error covariance matrix is derived as

$$\begin{aligned}\boldsymbol{P}_{k+1/k} &= E\left[(\boldsymbol{\Phi}_k\mathbf{e}_{k/k} + \mathbf{W}_k)(\boldsymbol{\Phi}_k\mathbf{e}_{k/k} + \mathbf{W}_k)^\mathrm{T}\right]\\ &= \Phi_k\boldsymbol{P}_{k/k}\Phi_k^\mathrm{T} + \boldsymbol{Q}_k\,.\end{aligned} \tag{44.19}$$

According to the above statements, we can make several remarks about Kalman estimation:

1. Since $\boldsymbol{K}_\mathrm{k}$ is optimal, the posterior estimate $\hat{\boldsymbol{X}}_{k/k}$ is an optimal estimate.
2. Based on (44.12), (44.15), (44.16), (44.17) and (44.19), recursive steps for constructing a one-step estimator are summarized in Fig. 44.4.
3. The recursive loop involves two different kinds of updating. Equations (44.12) and (44.16) yielding $\hat{\boldsymbol{X}}_{k/k}$ and $\boldsymbol{P}_{k/k}$ from $\hat{\boldsymbol{X}}_{k/k-1}$ and $\boldsymbol{P}_{k/k-1}$ are measurement updates; Equations (44.17) and (44.19) projecting $\hat{\boldsymbol{X}}_{k/k}$ and $\boldsymbol{P}_{k/k}$ to $\hat{\boldsymbol{X}}_{k+1/k}$ and $P_{k+1/k}$ are time updates.
4. The initial conditions, i.e. $\hat{X}_{0/-1}$, $P_{0/-1}$, Φ_0, H_0, Q_0, and R_0 have to be known before we can start the recursive steps.

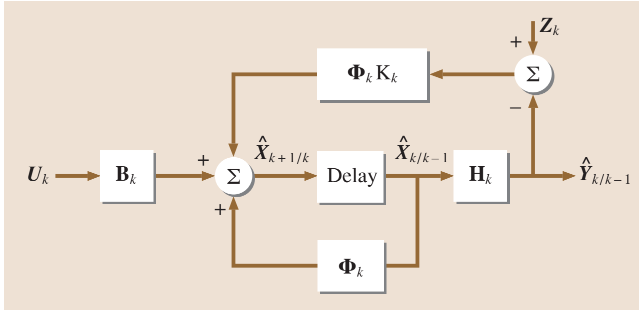

Fig. 44.3 Block diagram of a Kalman filter

44.2.3 Prediction

The estimate resulting from the recursive steps in Fig. 44.4 is a one-step-ahead prediction. Based on the posterior estimate (44.12), the state that is N steps ahead of the measurement $\boldsymbol{Z}_k$ can be predicted by using the ARMA (autoregressive and moving average) model [44.16]. From (44.17) and (44.19), the equations for N-step-ahead prediction are derived as

$$\begin{aligned}\hat{\boldsymbol{X}}_{k+N/k} &= \left(\prod_{i=k+N-1}^{k}\Phi_i\right)\hat{\boldsymbol{X}}_{k/k}\\ &\quad + \sum_{m=k}^{k+N-2}\left[\left(\prod_{i=k+N-1}^{m+1}\Phi_i\right)\boldsymbol{B}_m\boldsymbol{U}_m\right]\\ &\quad + \boldsymbol{B}_{k+N-1}\boldsymbol{U}_{k+N-1}\,,\end{aligned} \tag{44.20}$$

$$\begin{aligned}P_{k+N/k} &= \left(\prod_{i=k+N-1}^{k}\Phi_i\right)\boldsymbol{P}_{k/k}\left(\prod_{j=k}^{k+N-1}\Phi_j^\mathrm{T}\right)\\ &\quad + \sum_{m=k}^{k+N-2}\left[\left(\prod_{i=k+N-1}^{m+1}\Phi_i\right)Q_m\right.\\ &\quad \left.\times\left(\prod_{j=m+1}^{k+N-1}\Phi_j^T\right)\right] + Q_{k+N-1}\,.\end{aligned} \tag{44.21}$$

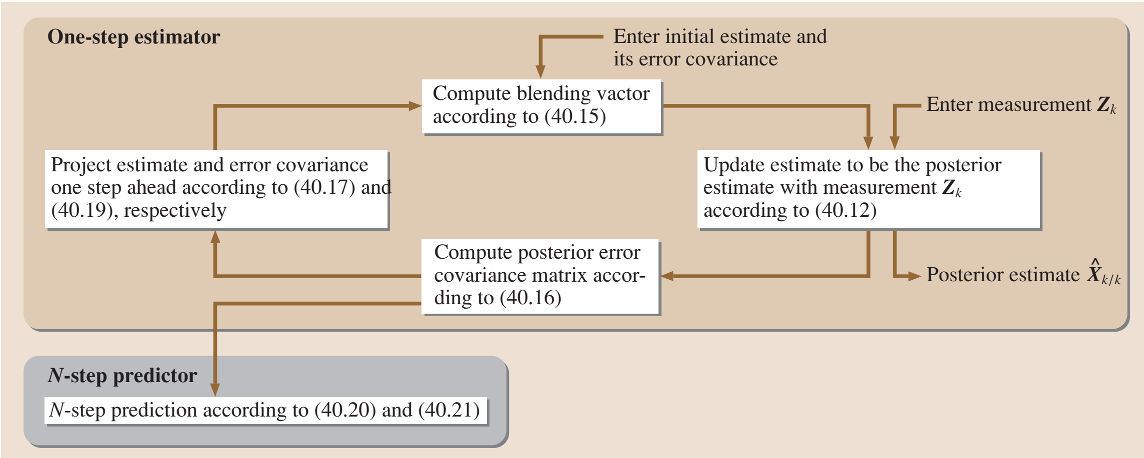

Fig. 44.4 One-step estimator and N-step predictor

The N-step predictor is an appendage of the one-step estimation loop [44.16]. It is also shown in Fig. 44.4. Since the current predicted value is assumed to be the initial value for the next prediction, the more steps the predictor predicts, the larger the error.

44.3 Armature-Controlled DC Motor

An armature-controlled DC motor is employed in this section as the physical model on which to perform failure prediction. The motor circuit representation is shown in Fig. 44.5.

44.3.1 Transfer Function

Using the properties of a DC motor, the following equations can be formulated [44.17]:

$$\phi = k_f i_f \,, \tag{44.22}$$

$$\begin{aligned} T &= \frac{ZP}{2\pi a}\phi i_a \\ &= k_1 (k_f i_f)\, i_a \\ &= k_T i_a \end{aligned} \tag{44.23}$$

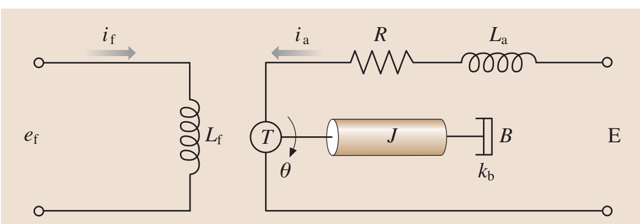

Fig. 44.5 Circuit representation of DC motor

$$e_b = k_b \frac{d\theta}{dt} \,, \tag{44.24}$$

$$L_a \frac{d}{dt} i_a + R i_a + e_b = E \,, \tag{44.25}$$

$$J\ddot{\theta} + B\dot{\theta} = T \,, \tag{44.26}$$

where $k_1 = \frac{ZP}{2\pi a}$ is called the motor constant, and $k_T = k_1 (k_f i_f)$ is the motor torque constant.

Taking the Laplace transform for (44.24), (44.25) and (44.26) results in

$$E_b(s) = k_b s\theta(s) \,, \tag{44.27}$$

$$(L_a s + R) I_a(s) = E(s) - E_b(s) \,, \tag{44.28}$$

$$(Js^2 + Bs)\theta(s) = T(s) = k_T I_a(s) \,. \tag{44.29}$$

Combining (44.27), (44.28) and (44.29), the transfer function of a DC motor is derived as

$$\frac{\theta(s)}{E(s)} = \frac{k_T}{s\left[(sL_a + R)(sJ + B) + k_T k_b\right]} \,. \tag{44.30}$$

Accordingly, the block diagram of a DC motor is as shown in Fig. 44.6. If $L_a \approx 0$, (44.30) can be rewritten as

$$\frac{\theta(s)}{E(s)} = \frac{k_m}{s(s\tau_m + 1)} \,, \tag{44.31}$$

where $k_\mathrm{m} = \frac{k_\mathrm{T}}{RB+k_\mathrm{T}k_\mathrm{b}}$ and $\tau_\mathrm{m} = \frac{RJ}{RB+k_\mathrm{T}k_\mathrm{b}}$ are called the motor gain constant and the motor time constant, respectively.

44.3.2 Continuous State Space Model

Define θ, $\dot{\theta}$, and i_a as state variables, so that the state vector is $\boldsymbol{X} = [\theta\,\dot{\theta}\,i_\mathrm{a}]^\mathrm{T}$.

Since

$$\frac{\mathrm{d}}{\mathrm{d}t}\theta = \dot{\theta}\,, \tag{44.32}$$

substituting (44.23) and (44.32) into (44.26) yields

$$\frac{\mathrm{d}}{\mathrm{d}t}\dot{\theta} = \frac{1}{J}\left(k_\mathrm{T}i_\mathrm{a} - B\dot{\theta}\right) = \frac{k_\mathrm{T}}{J}i_\mathrm{a} - \frac{B}{J}\dot{\theta}\,. \tag{44.33}$$

Moreover, substituting (44.24) into (44.25) yields

$$\frac{\mathrm{d}}{\mathrm{d}t}i_\mathrm{a} = \frac{1}{L_\mathrm{a}}\left(E - Ri_\mathrm{a} - e_\mathrm{b}\right) = \frac{E}{L_\mathrm{a}} - \frac{k_\mathrm{b}}{L_\mathrm{a}}\dot{\theta} - \frac{R}{L_\mathrm{a}}i_\mathrm{a}\,. \tag{44.34}$$

During measurement, the rotation speed $\dot{\theta}$ is the motor output. According to (44.32), (44.33) and (44.34), the continuous state equations of the DC motor are

$$\frac{\mathrm{d}}{\mathrm{d}t}\begin{pmatrix}\theta\\ \dot{\theta}\\ i_\mathrm{a}\end{pmatrix} = \begin{pmatrix}0 & 1 & 0\\ 0 & -\frac{B}{J} & \frac{k_\mathrm{T}}{J}\\ 0 & -\frac{k_\mathrm{b}}{L_\mathrm{a}} & -\frac{R}{L_\mathrm{a}}\end{pmatrix}\begin{pmatrix}\theta\\ \dot{\theta}\\ i_\mathrm{a}\end{pmatrix} + \begin{pmatrix}0\\ 0\\ \frac{1}{L_\mathrm{a}}\end{pmatrix}E\,, \tag{44.35}$$

$$Y = \begin{pmatrix}0 & 1 & 0\end{pmatrix}\begin{pmatrix}\theta\\ \dot{\theta}\\ i_\mathrm{a}\end{pmatrix}\,. \tag{44.36}$$

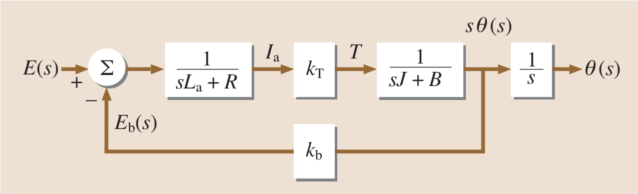

Fig. 44.6 Block diagram of DC motor

44.3.3 Discrete State Space Model

The state equations for a continuous system take the form of [44.18]:

$$\begin{aligned}\dot{X}(t) &= A_\mathrm{c}X(t) + B_\mathrm{c}U(t)\\ Y(t) &= C_\mathrm{c}X(t) + D_\mathrm{c}U(t)\end{aligned} \tag{44.37}$$

Let $\Phi_\mathrm{c}(t) = L^{-1}[(s\mathbf{I} - \mathbf{A}_\mathrm{c})^{-1}]$ be the state transition matrix for (44.37). The discrete state equations sampled from (44.37) by a sample-and-hold with a time interval of T seconds are as follows [44.19]:

$$\begin{aligned}\boldsymbol{X}_{k+1} &= \mathbf{A}\boldsymbol{X}_k + \mathbf{B}\boldsymbol{U}_k\,,\\ \boldsymbol{Y}_k &= \mathbf{C}\boldsymbol{X}_k + \mathbf{D}\boldsymbol{U}_k\,,\end{aligned}$$

where

$$\mathbf{A} = \Phi_\mathrm{c}(T)\,, \tag{44.38}$$

$$\mathbf{B} = \left[\int_0^T \Phi_\mathrm{c}(\tau)\,\mathrm{d}\tau\right]B_\mathrm{c}\,, \tag{44.39}$$

$$\boldsymbol{C} = \boldsymbol{C}_\mathrm{c}\,, \tag{44.40}$$

$$\boldsymbol{D} = \boldsymbol{D}_\mathrm{c}\,. \tag{44.41}$$

44.4 Simulation System

This section describes a computer simulation of failure prediction for PM on a DC motor.

44.4.1 Parameters

The parameters used for the DC motor in this simulation are: follows [44.20]:

$E = 10\,\mathrm{V}$,
$B = 0.001\,\mathrm{N\,m\,s}$,
$J = 0.01\,\mathrm{kg\,m^2}$,
$K_\mathrm{T} = 1\,\mathrm{N\,m\,/\,A}$,
$K_\mathrm{b} = 0.02\,\mathrm{V\,s}$,
$R = 10\,\Omega$,
$L_\mathrm{a} = 0.01\,\mathrm{H}$.

Substituting them into (44.35) and (44.36), the continuous state equations of the motor become

$$\frac{\mathrm{d}}{\mathrm{d}t}\begin{pmatrix}\theta\\ \dot{\theta}\\ i_\mathrm{a}\end{pmatrix} = \begin{pmatrix}0 & 1 & 0\\ 0 & -0.1 & 100\\ 0 & -2 & -1000\end{pmatrix}\begin{pmatrix}\theta\\ \dot{\theta}\\ i_\mathrm{a}\end{pmatrix} + \begin{pmatrix}0\\ 0\\ 100\end{pmatrix}10\,, \tag{44.42}$$

$$Y = \begin{pmatrix}0 & 1 & 0\end{pmatrix}\begin{pmatrix}\theta\\ \dot{\theta}\\ i_\mathrm{a}\end{pmatrix}\,. \tag{44.43}$$

The following parameters are also used to predict failure:

1. The failure threshold of the motor is defined as 5% less than the normal value, which is set to be the

initial estimate in the Kalman prediction procedure. That is, the motor is judged to fail if the rotation speed drops to 95% of the normal value.

2. Mean time between failure (MTBF) for the motor is 100 000 h [44.21].
3. Sampling interval T is 1 h (this is the increment time for every step in Kalman prediction).
4. Disturbance $\boldsymbol{W}_k$ has mean 0 and variance 0.01 V [44.22].
5. Measurement error $\boldsymbol{V}_k$ for $\dot{\theta}$ has a zero mean and a standard deviation of 3.333 rad/s, which is 1% of the full-scale accuracy [44.23] of the measurement.
6. PM lead-time is set to $n \times 60$ min, where n is the number of steps ahead in the prediction. Accordingly, the alarm signal is activated (to indicate that PM should be executed) whenever the Kalman filter predicts that the motor speed will be lower than the prescribed threshold $n \times 60$ min later.

44.4.2 Monte Carlo Simulation and ARMA Model

Assuming that motor failures occur randomly, a Monte Carlo simulation (MCS) can be used to generate the failure times of the motor. The relationship between the failure rate $h(t)$ and the distribution function of the lifetime $f(t)$ is [44.5]

$$f(t) = h(t) \exp\left[-\int_0^t h(\tau)\,\mathrm{d}\tau\right] . \tag{44.44}$$

Failures occur randomly during the useful lifetime, statistically conforming to a bathtub curve [44.5]. The failure rate is constant during this period. Let the failure rate in (44.44) be a constant λ, and so (44.44) becomes

$$f(t) = \lambda \exp\left(-\int_0^t \lambda\,\mathrm{d}\tau\right) = \lambda\,\mathrm{e}^{-\lambda t} , \tag{44.45}$$

which is an exponential distribution function. Let u_i, $i = 1, 2, 3, \ldots, m$, represent a set of standard uniformly distributed random numbers. The corresponding numbers t_i of the random variable t in (44.45) (in other words the simulated failure times), are written as [44.5]

$$t_i = -\frac{1}{\lambda} \ln u_i , \tag{44.46}$$

with exponential distributions.

The measurements needed for the recursive estimation loop of the Kalman filter, as depicted in Fig. 44.4, are generated by the ARMA model ((44.1) to (44.3)). Simulations in this section are performed using MATLAB [44.24]. All random numbers and white sequences with prescribed variances needed are obtained using the random number generator in MATLAB.

44.4.3 Exponential Attenuator

To account for the aging failure modes and the exponentially distributed failure times t_i, an exponential attenuator, represented by $\mathrm{e}^{-t/\tau}$, is placed at the output ends of both the motor system and the Kalman filter. The block diagram of the simulation system is shown in Fig. 44.7. The symbol τ of the attenuator in Fig. 44.7 denotes the failure time constant of the motor, which varies with the failure times that are generated by the MCS.

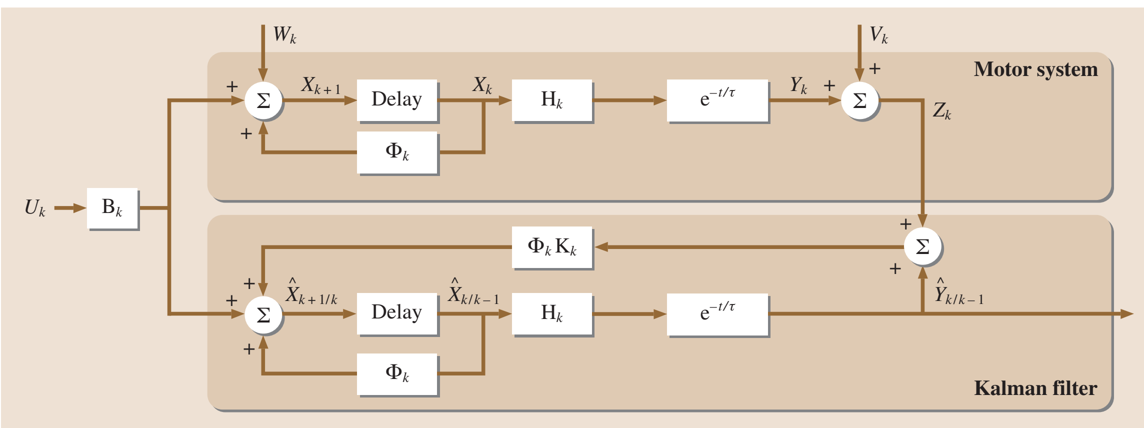

Fig. 44.7 Block diagram of the simulation system

44.4.4 Simulation Results

Two categories of simulation are conducted in this section, namely one-step-ahead prediction and two-steps-ahead prediction. According to the central limit theorem (CLT), estimators follow the normal distribution if the sample size is sufficiently large. A sample size of 30 is a reasonable number to use [44.25]. The larger the sample size, the smaller the estimated error, which tends to zero when the sample size approaches infinity. Hence, each simulation is executed 100 times. Simulation results for a lead-time of 60 min – one-step-ahead prediction – is shown in Fig. 44.8. Figure 44.8a shows the results for the 100 simulations of failure times generated by the MCS, the failure times predicted by the Kalman filter, and the associated alarm times. Figure 44.8b shows the results from one of the 100 simulations with properly scaled coordinates. The failure time differences between MCS and Kalman prediction are shown in Fig. 44.9. The mean value and the standard deviation of the differences in the 100 simulations are −34.71 min and 65.90 min, respectively. The negative sign of the mean value indicates that the failure time predicted by the Kalman filter occurs earlier than the time generated by MCS. According to the Z formula [44.25], the error in estimating the mean value of the sample population can be calculated by

$$E_r^2 = \frac{Z_{\alpha/2}^2 \sigma^2}{n} \,.$$

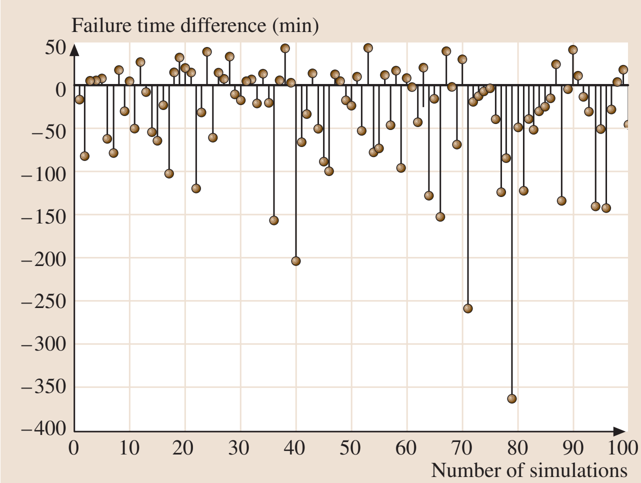

Fig. 44.9 Differences between the failure times given by Monte Carlo simulation results and Kalman filter predictions when the lead-time = 60 min

The Z value for a 99% confidence level is 2.575 [44.25]. Solving for E_r gives

$$E_r = \frac{(2.575)(65.8954)}{\sqrt{100}} = 16.97(\text{min}) \,.$$

According to the above data, we can say with 99% confidence that the mean value of the time difference between the MCS and the Kalman prediction is −34.71 ± 16.97 min, in other words from −17.74 min to −51.68 min. Taking the time difference into account,

Part E | 44.4

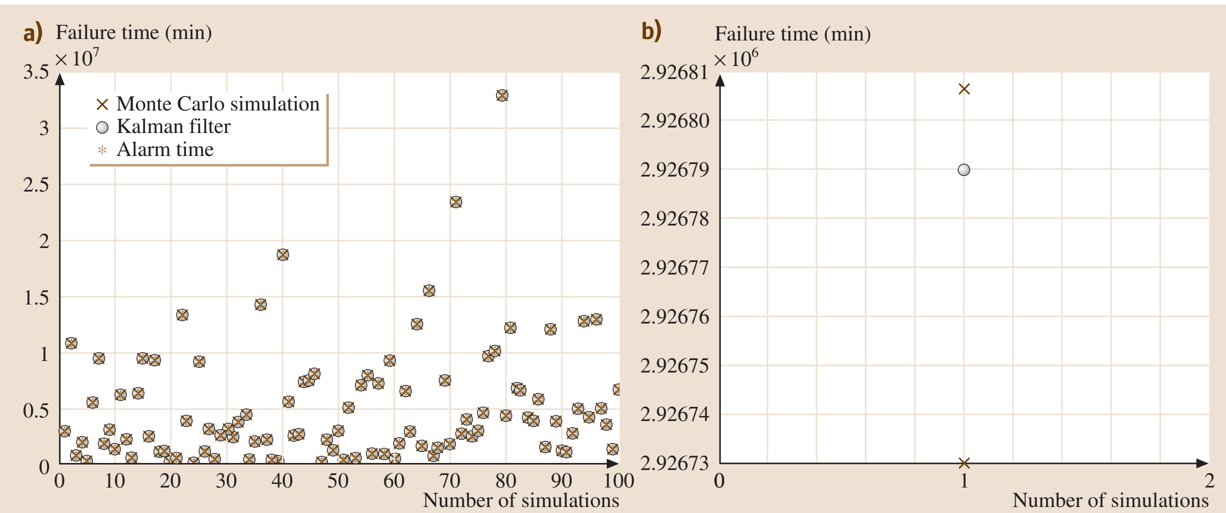

Fig. 44.8 Failure times generated by Monte Carlo simulation and predicted by Kalman filter when lead-time = 60 min

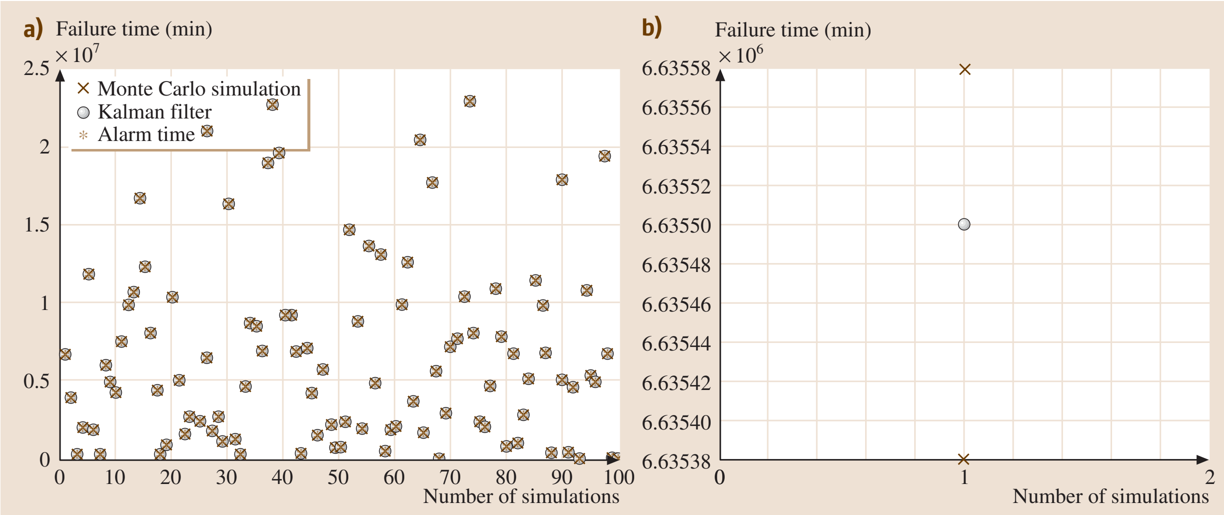

Fig. 44.10 Failure times generated by Monte Carlo simulation and predicted by Kalman filter when the lead-time = 120 min

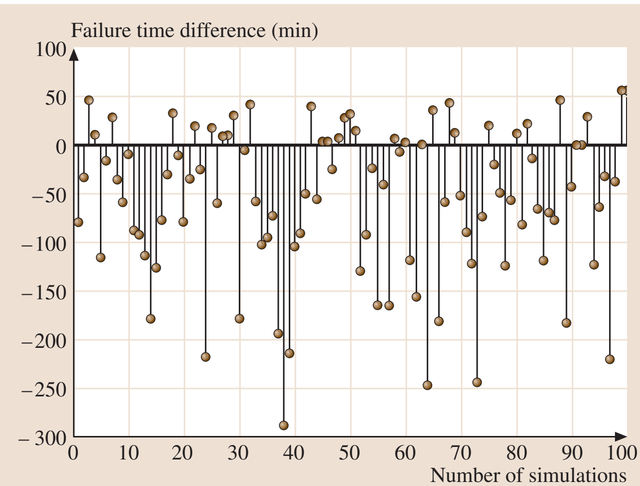

Fig. 44.11 Differences between the failure times given by Monte Carlo simulation results and Kalman filter predictions when the lead-time = 120 min

the alarm signal will appear at least 77.74 min prior to failure occurrence.

The results for the second category of simulation, – two-steps-ahead prediction, with a PM lead-time of 120 min – are shown in Figs. 44.10 and 44.11. The mean value of the difference in failure times from the MCS and the Kalman prediction is −56.34 min, and the 99% confidence interval for this mean is 20.06 min. The maximum prediction error for this case is 76.40 min, which is 1.48 times greater than the error from the one-step-ahead prediction.

44.4.5 Notes About the Simulation

1. In order to avoid false alarms, the failure threshold should not be set too close to the normal value. Otherwise, a decision-making algorithm is needed to identify that a failure has actually been predicted.
2. The disturbance amplitude should comprise all possible uncertainties about the motor and the environment.
3. The proposed method cannot deal with abrupt changes during a sampling interval. Thus, the sampling interval should not be too long.
4. Since the prediction is made for purposes of PM, the prediction time should be long enough that PM can be performed before the failure occurs.
5. In contrast to the deterministic portion, the variance that is driven by the disturbance of the system is small. The difference in state variables between prediction steps fades very rapidly. Thus, using the N-step predictor ((44.20)), only the prediction for the first few steps is of significance.
6. The proposed method in this section is exemplified by a motor system, which is treated as a component. The procedure can be executed on a multicomponent system if state equations can be constructed for the components as a whole. The procedure can be performed on either the multicomponent system or each of the components.

For a complicated or large system, the proposed method can be only performed on those elements that are present in minimum cut sets as constructed by fault tree analysis or a Petri net model for failure [44.26].

7. Multiple failure modes can be modeled as modules, such as an attenuator for simulating an aging failure mode for the electrical motor exemplified in this paper, and placed at the system model output end to extend the proposed method. As described previously, the system model may be single-component or multicomponent. System failure analysis can determine whether the failure modules occur in series, parallel or in other arrangements [44.26]. As for a multicomponent system with multiple failure modes, the system can be split into several components and the related failure module(s) placed at the output end of each component in order to perform state estimation using the Kalman filter for each component.

44.5 Armature-Controlled DC Motor Experiment

This section presents a PM failure-prediction experiment for a DC motor.

44.5.1 Experiment Design

The experiment design, shown in Fig. 44.12, comprises a DC motor with a driver unit and a data acquisition system.

DC Motor

The DC motor used in this experiment is made by TECO, Taiwan. The model number of the motor is GSDT-1/2 hp. Parameters for the DC motor used in this study are as follows [44.27]:

$E = 150\,\mathrm{V}$, $B = 0.001\,135\,\mathrm{N\,m\,s}$, $J = 0.0102\,\mathrm{kg\,m^2}$, $K_\mathrm{T} = 0.153\,\mathrm{N\,m/A}$, $K_\mathrm{b} = 1.926\,\mathrm{V\,s}$, $R = 3.84\,\Omega$, $L_\mathrm{a} = 0.01\,\mathrm{H}$.

Substituting these into (44.35) and (44.36), the continuous state equations of the motor become

$$\frac{\mathrm{d}}{\mathrm{d}t}\begin{pmatrix}\theta\\ \dot\theta\\ i_\mathrm{a}\end{pmatrix} = \begin{pmatrix}0 & 1 & 0\\ 0 & -0.111 & 15\\ 0 & -192.6 & -384\end{pmatrix}\begin{pmatrix}\theta\\ \dot\theta\\ i_\mathrm{a}\end{pmatrix} + \begin{pmatrix}0\\ 0\\ 100\end{pmatrix} 150\,, \tag{44.47}$$

$$Y = \begin{pmatrix}0 & 1 & 0\end{pmatrix}\begin{pmatrix}\theta\\ \dot\theta\\ i_\mathrm{a}\end{pmatrix}\,. \tag{44.48}$$

The discrete state equations sampled from (44.47) and (44.48) with a time interval of $T = 1200\,\mathrm{s}$ are

$$\begin{pmatrix}\theta_{k+1}\\ \dot\theta_{k+1}\\ i_{\mathrm{a},k+1}\end{pmatrix} = \begin{pmatrix}1 & 0.13098 & 0.0051164\\ 0 & 0 & 0\\ 0 & 0 & 0\end{pmatrix}\begin{pmatrix}\theta_k\\ \dot\theta_k\\ i_{\mathrm{a},k}\end{pmatrix} + \begin{pmatrix}613.91\\ 0.51164\\ 0.0037955\end{pmatrix} 150\,, \tag{44.49}$$

$$Y_k = \begin{pmatrix}0 & 1 & 0\end{pmatrix}\begin{pmatrix}\theta_k\\ \dot\theta_k\\ i_{\mathrm{a},k}\end{pmatrix}\,. \tag{44.50}$$

The following parameters are also used to estimate state in this experiment:

1. Sampling interval $T = 20\,\mathrm{min}$, which is the increment time for each of the steps used in Kalman prediction. In order to compare results for shorter and longer T's, another two estimations with different time intervals, $T = 5\,\mathrm{min}$ and $T = 60\,\mathrm{min}$ were tested.
2. Disturbance $\boldsymbol{W}_k$ has a mean of zero and a variance of 0.1 V [44.22].

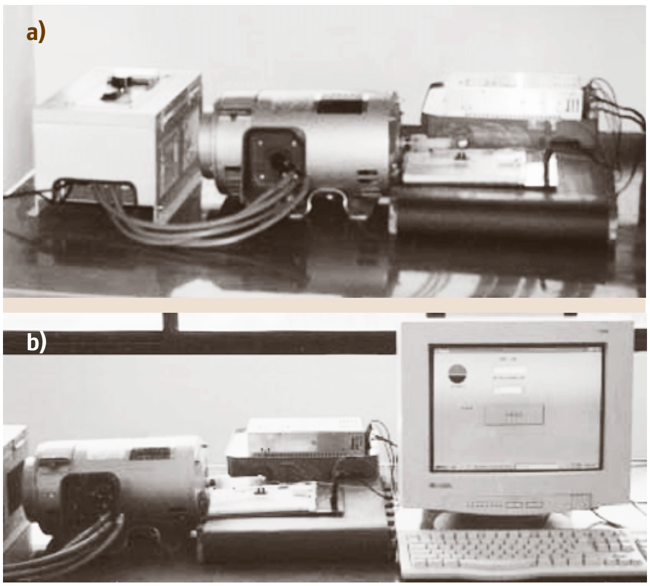

Fig. 44.12 Experiment set-up

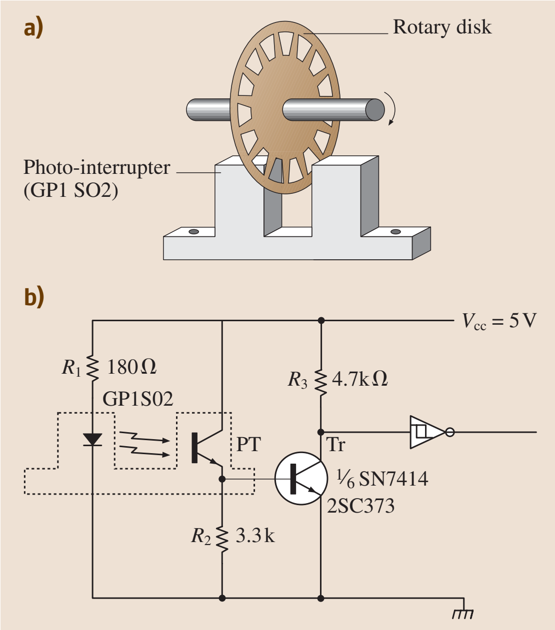

Fig. 44.13 Device and circuit for rotating speed measurement

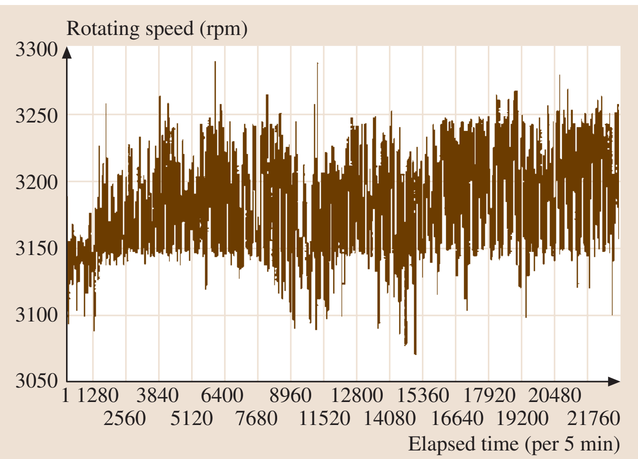

Fig. 44.14 Rotating speed measurements, taken every 5 min

3. The measurement error $\boldsymbol{V}_k$ for $\dot{\theta}$ has a mean of zero and an accuracy of 1% [44.23] of the full-scale measurement.
4. The rated rotation speed of the DC motor is 3180 rpm [44.27], which is therefore the initial value of the state variable $\dot{\theta}$.

Data Acquisition System

The data acquisition system used in this experiment comprises a photo-interrupter circuit, a personal computer (PC), and a RS-232 transmission interface [44.23]. The rotation speed of the DC motor is measured by the photo-interrupter coded GP1S02. The shaft of a rotary disk is connected to the shaft of the DC motor, and the disk is placed between the light-emitting element and the light-receiving element of the photo-interrupter so as to generate pulse-signals while the motor rotates. The device and the circuit are shown in Fig. 44.13.

Pulse-signals are transmitted to the PC through the RS-232 interface, and the PC counts the pulses that are accumulated within 60 seconds in order to derive the rotation speed in rpm (revolution per minute).

44.5.2 Experimental Results

The results of the experiment are presented and discussed in this section.

Measured Data

The rotation speed of the motor was measured and recorded every 5 min day and night for 80 d. Because the experiment lasted for nearly three months, lots of data were accumulated. There are 288 measurements per day and 23 040 data values in total for that period of time. Figure 44.14 shows the results. The data were fed into the estimator, as depicted in Fig. 44.14, in order to estimate the one-step-ahead state variables. The measured data and the resulting estimates for $T = 20$ min (every fourth measurement is used) are shown in Fig. 44.15. The data would be difficult to interpret if all 23 040 of the data values were shown in one chart. To avoid this and therefore to present the results more clearly, the unit used on the time axis of Fig. 44.15 is set to be 24 h (one point per day).

Error in the Estimate

The error in the estimate (in percent) is defined as

$$E_r\% = \frac{\hat{\dot{\theta}}_{k+1/k} - \dot{\theta}_{k+1}}{\dot{\theta}_{k+1}} \times 100\% \,. \tag{44.51}$$

E_r represents the difference between the predicted value and the actual value. Figure 44.16 shows the results obtained from (44.51) using the data in Fig. 44.15. Reading from Fig. 44.16, the maximum $E_r\%$ is less than 3%.

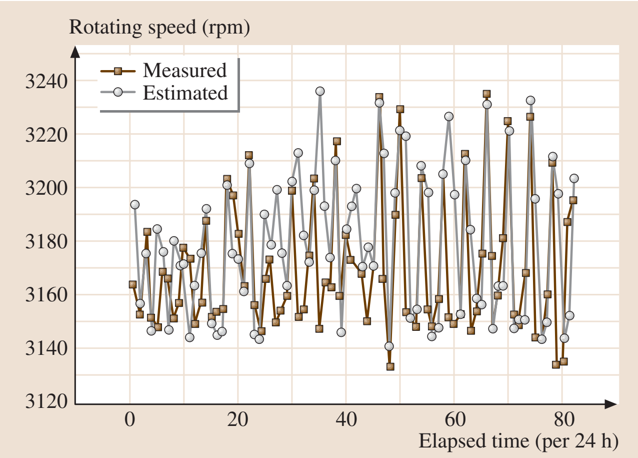

Fig. 44.15 Measured and estimated motor rotating speeds

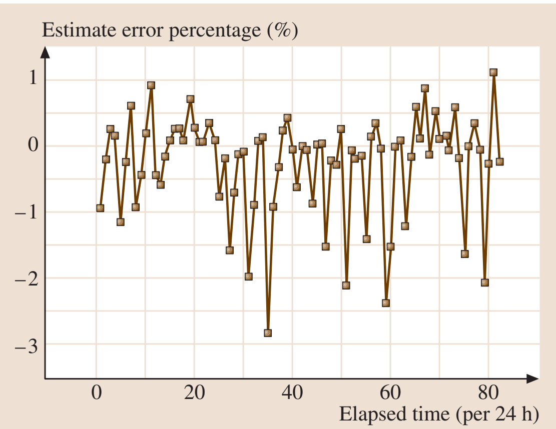

Fig. 44.16 Percent errors in estimates

Mean Value and Variance of the Accuracy of the Estimate

Let

$$X_i = 1 - E_r\%_i \quad i = 1, 2, \ldots, 23\,040 \tag{44.52}$$

be the individual accuracy of each estimate, and

$$\mu = \frac{\sum_{i=1}^{23\,040} X_i}{23040}\,, \tag{44.53}$$

$$\sigma^2 = \frac{\sum_{i=1}^{23\,040} (X_i - \mu)^2}{23\,040} \tag{44.54}$$

be the mean value and the variance [44.25] of the accuracy for the 23 040 samples, respectively. The resulting mean values, variances, and standard deviations (σ) for the estimated accuracy for $T = 5, 20, 60$ min, obtained using (44.52), (44.53), and (44.54), are summarized in Table 44.1.

Table 44.1 Mean values, standard deviations, and variances for different T

T min	μ(%)	σ(%)	σ^2(%)
5	99.74656	0.402957	0.162374
20	99.74060	0.471612	0.222418
60	99.72771	0.652469	0.425716

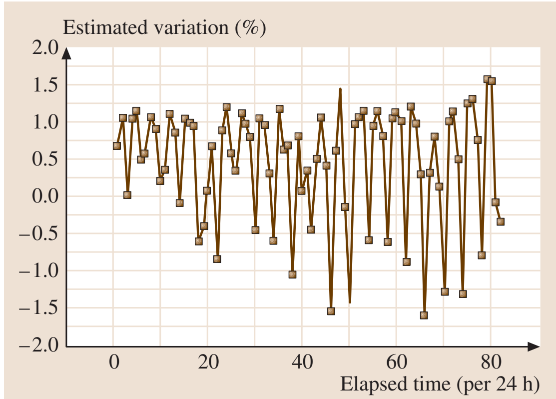

Fig. 44.17 Percent variation in the estimated rotating speed

Variation in Rotation Speed

The variation in estimated rotation speed for the DC motor (in percent) is defined using

$$V\% = \frac{\hat{\hat{\theta}}_{k+1/k} - 3180}{3180} \times 100\%\,. \tag{44.55}$$

$V\%$ represents the percentage variation in the estimated rotation speed from the rated value 3180 rpm; in other words the abnormality in the motor's performance. It is used to judge whether the motor is going to fail or not. Since the MTBF of the motor is about 100 000 h [44.21], the rotation speed of the motor in this experiment varied by less than 2% of the rated value over the experiment time period. The percentage variation in the estimated rotation speed of the DC motor is shown in Fig. 44.17.

44.5.3 Notes About the Experiment

1. The mean accuracies of the estimates for $T = 5$, 20, and 60 min were all higher than 99.7%, which infers that the one-step-ahead state variable can be accurately predicted using the proposed method.

2. A threshold is a value used to judge whether or not an equipment failure occurs. It is defined as the measurement value that is taken just prior to or at the time of failure [44.28]. For failure prediction, the threshold for the motor should be determined by the user of the motor according to requirements of the specific situation. Once the estimated value reaches the threshold, a failure is predicted.
3. The disturbance amplitude should encompass all possible uncertainties for the motor and the environment.
4. Since the prediction is used for the purposes of PM, the prediction time should be long enough that PM can be performed before failure occurs.
5. The method proposed in this study is exemplified by a motor system, which is treated as a component. The procedure can be performed on a multicomponent system if state equations can be constructed for the components as a whole. It is feasible to perform the procedure on either the multicomponent system or each of the components. For a complicated or large system, the proposed method can be performed on those elements present in minimum cut sets as constructed by fault tree analysis or the Petri net model for failure [44.26].

44.6 Conclusions

Knowing when and where a system needs maintenance and economizing capital investment are two of the major issues associated with maintenance. The proposed scheme optimizes maintenance in the following aspects:

1. Before a system failure occurs, the scheme is able to indicate where and when the failure is going to be.
2. It makes the health of the system and its historical record clear at a glance.
3. Scheduled maintenance is performed according to a statistical average, which still retains an unavoidable risk that the system may fail before the criteria are exceeded, so a failure may occur unexpectedly. On the other hand, the actual duty cycles for a certain part or module may be longer than the average, so it is a waste of investment if they are replaced during scheduled maintenance. The condition-based scheme avoids those drawbacks.

Failure prediction simulation and experiment for PM, performed via state estimation using Kalman filtering, was described in this chapter. In contrast to previous works, this study uses Kalman filtering instead of parameter trends to predict the time of failure and to determine the PM execution time. The resulting prediction errors are acceptable for not only one-step-ahead prediction but also two-steps-ahead prediction. To simulate the aging failure mode, a state variable – the rotation speed – is monitored in the simulation. More measured variables mean that more complicated failure modes can be simulated. Moreover, the chapter also described an experiment on a DC motor used for state estimation via predictive maintenance using the Kalman filter. The resulting prediction errors for one-step-ahead prediction were acceptable. The shorter the increment time for Kalman prediction, the higher the prediction accuracy. Considerations used to determine the PM lead-time and the increment time required for prediction contradict each other. How to work out a compromise and end up with an optimal value is an important issue. By incorporating fault tree analysis or a Petri net model for failure, the proposed method can be performed on only those elements of a complicated or large system that fall into minimum-cut sets instead of all of the elements of the system. Therefore, failure can be prevented in enough time to promote reliability if state estimation using the Kalman filter is applied to predictive maintenance.

References

44.1 E. A. Elsayed: *Reliability Engineering* (Addison Wesley, Reading 1996)

44.2 J. D. Patton, Jr.: *Preventive Maintenance* (Instrument Soc. Am., Research Triangle Park 1983)

44.3 IEV: *International Electrotechnical Vocabulary (IEV); Chapt. 191: Dependability and quality of service* (International Electrotechnical Commission, Geneva 1990)

44.4 M. Rausand, K. Oien: The basic concept of failure analysis, Reliab. Eng. Syst. Safe. **53**, 73–83 (1996)

44.5 S. S. Rao: *Reliability-Based Design* (McGraw-Hill, New York 1992)

44.6 O. T. Ogunyemi, P. I. Nelson: Prediction of Gamma failure times, IEEE Trans. Reliab. **46**(3), 400–405 (1997)
44.7 W. Nelson: Weibull prediction of a future number of failures, Qual. Reliab. Eng. Int. **16**, 23–26 (2000)
44.8 E. A. Rietman, M. Beachy: A study on failure prediction in a plasma reactor, IEEE Trans. Semiconduct. M. **11**(4), 670–680 (1998)
44.9 S. N. Kher, G. M. Bubel: Predicting system-failure risk from unanticipated fiber-breaks in manufacturing, IEEE Trans. Reliab. **47**(2), 126–130 (1998)
44.10 R. Isermann: Process fault detection based on modeling and estimation methods – A survey, Automatica **20**(4), 387–404 (1984)
44.11 J. L. Tylee: On-line failure detection in nuclear power plant instrumentation, IEEE Trans. Automat. Contr. **AC-28**(3), 406–415 (1983)
44.12 M. M. Sidar, B. F. Doolin: On the feasibility of real-time prediction of aircraft carrier motion at sea, IEEE Trans. Automat. Contr. **AC-28**(3), 350–355 (1983)
44.13 R. F. Berg: Estimation and prediction for maneuvering target trajectories, IEEE Trans. Automat. Contr. **AC-28**(3), 294–304 (1983)
44.14 B. D. O. Anderson, J. B. Moore: *Optimal Filtering* (Prentice-Hall, Englewood Cliffs 1979)
44.15 A. S. Willsky: A survey of design methods for failure detection in dynamic systems, Automatica **12**, 601–611 (1976)
44.16 R. G. Brown, P. Y. C. Hwang: *Introduction to Random Signals and Applied Kalman Filtering* (Wiley, New York 1997) pp. 198–224 Sec. 5.3-5.6
44.17 K. Ogata: *Modern Control Engineering* (Prentice-Hall, Englewood Cliffs 1980)
44.18 C. L. Phillips, H. T. Nagle: *Digital Control System Analysis and Design* (Prentice-Hall, Englewood Cliffs 1990)
44.19 K. Ogata: *Discrete-Time Control Systems* (Prentice-Hall, Englewood Cliffs 1987)
44.20 G. F. Franklin, J. D. Powell, A. Emami-Naeini: *Feedback Control of Dynamic Systems* (Addison-Wesley, New York 1994)
44.21 B. S. Dhillon: *Mechanical Reliability: Theory, Models and Applications* (AIAA, Washington DC 1988)
44.22 C. Y. Chiang-Lin: *Parameter estimation and fault diagnosis on the thermal network by applying the extended Kalman filter and the expert system, M.S. Thesis* (National Chiao Tung University, Taiwan 1991)
44.23 J. G. Webster, R. Palla's-Areny: *Sensor and Signal Conditioning* (Wiley, New York 1991)
44.24 D. Fowley, M. Horton: *User's Guide to MATLAB, Version 4* (Prentice-Hall, Englewood Cliffs 1995)
44.25 K. Black: *Business Statistics, Contemporary Decision Making* (West Publ., Los Angeles 1997)
44.26 S. K. Yang, T. S. Liu: Failure analysis for an airbag inflator by Petri nets, Qual. Reliab. Eng. Int. **13**, 139–151 (1997)
44.27 TECO: *DC Motor, Universal Type: User Guide* (Tung-Yuang Electrical Machine Co. (TECO), Taipia 2001)
44.28 S.K. Yang, T.S. Liu: A Petri net approach to early failure detection and isolation for preventive maintenance, Qual. Reliab. Eng. Int. **14**, 319–330 (1998)